

---

# In Vivo Evidence of Endothelial Injury in Chronic Obstructive Pulmonary Disease by Lung Scintigraphic Assessment of $^{123}\text{I}$ -Metaiodobenzylguanidine

Tsuyoshi Arao, MD<sup>1</sup>; Noriaki Takabatake, MD<sup>1</sup>; Makoto Sata, MD<sup>1</sup>; Shuichi Abe, MD<sup>1</sup>; Yoko Shibata, MD<sup>2</sup>; Tsuguo Honma, MD<sup>3</sup>; Kazuei Takahashi<sup>3</sup>; Akio Okada<sup>3</sup>; Yasuchika Takeishi, MD<sup>1</sup>; and Isao Kubota, MD<sup>1</sup>

<sup>1</sup>First Department of Internal Medicine, Yamagata University School of Medicine, Yamagata, Japan; <sup>2</sup>Department of Laboratory Medicine, Yamagata University School of Medicine, Yamagata, Japan; and <sup>3</sup>Department of Radiology, Yamagata University School of Medicine, Yamagata, Japan

---

Scintigraphic evaluation of  $^{123}\text{I}$ -metaiodobenzylguanidine ( $^{123}\text{I}$ -MIBG) in the lungs is considered to recognize endothelial cell lesions. The aim of this study was to clarify the involvement of the pulmonary microvascular injury in the pathogenesis of chronic obstructive pulmonary disease (COPD). **Methods:** We investigated lung  $^{123}\text{I}$ -MIBG kinetics and clinical indices in 25 COPD patients and 12 control subjects. Mean uptake ratios of lung to mediastinum (L/M) were calculated in anterior planer images at 30 min (early image) and 270 min (delayed image) after intravenous injection of  $^{123}\text{I}$ -MIBG. Pulmonary mean wash-out rate (WR) of the  $^{123}\text{I}$ -MIBG was also calculated. **Results:** The L/M ratios in both early and delayed images of COPD patients, as well as its WR, were significantly lower than those of the control subjects (L/M early:  $1.26 \pm 0.18$  vs.  $1.54 \pm 0.11$ ,  $P < 0.0001$ ; L/M delayed:  $1.20 \pm 0.12$  vs.  $1.33 \pm 0.09$ ,  $P < 0.001$ ; WR:  $27.4\% \pm 5.3\%$  vs.  $34.2\% \pm 5.7\%$ ,  $P < 0.01$ ). There were significant relationships between lung WR of the  $^{123}\text{I}$ -MIBG and other diagnostic tests for the severity of COPD, such as forced expiratory volume in 1 s (% FEV<sub>1.0</sub>:  $r = 0.386$ ,  $P < 0.05$ ), carbon monoxide diffusing capacity/alveolar volume (DL<sub>CO</sub>/V<sub>A</sub>:  $r = 0.449$ ,  $P < 0.01$ ), arterial blood oxygen pressure (PaO<sub>2</sub>:  $r = 0.474$ ,  $P < 0.01$ ), alveolar-arterial oxygen tension gradient [A-a]DO<sub>2</sub> ( $r = -0.446$ ,  $P < 0.01$ ), and percentage of low-attenuation area ( $r = -0.458$ ,  $P < 0.01$ ) in the study population. **Conclusion:** Because lung WR of the  $^{123}\text{I}$ -MIBG is considered to be independent of an alteration of the pulmonary vascular surface area, these results suggest that the microvascular endothelial cell injury plays a significant role in the pathogenesis of COPD.

**Key Words:** chronic obstructive pulmonary disease;  $^{123}\text{I}$ -metaiodobenzylguanidine; microvascular endothelial cell injury

**J Nucl Med 2003; 44:1747-1754**

**C**hronic obstructive pulmonary disease (COPD) is a major cause of morbidity and mortality worldwide. In a recent review of the global burden of human illness, COPD ranked twelfth as a cause of lost quantity and quality of life and was projected to rank fifth by the year 2020 (1,2). This life-threatening disease is caused by proteolytic destruction of the lung parenchyma, resulting in enlargement of air spaces (emphysematous change) and loss of lung elasticity, as well as by chronic inflammatory narrowing of peripheral airways and mucus hypersecretion (3,4). Although chronic cigarette smoking is the most important risk factor for this global health issue, the underlying mechanisms that can account for these pathologic findings have not been fully understood.

Several previous studies to clarify the pathogenesis of COPD have preferably linked an active inflammatory process and progressive proteolytic injury of lung tissue with the protease-antiprotease or oxidant-antioxidant imbalance hypothesis (3,4). In short, alveolar macrophages and airway epithelial cells activated by cigarette smoke and other irritants release neutrophil-chemotactic factors, such as leukotriene B<sub>4</sub> and interleukin-8. Neutrophils and macrophages then release multiple proteinases and reactive oxygen species, which break down connective tissue in the lung parenchyma, stimulate mucus secretion, and induce air-space epithelial injury (3,4). However, one of the hazardous pitfalls of these approaches is that underlying mechanisms for the development of COPD tend to be recognized as processes occurring in favor of the alveolar side, but not in the pulmonary microcapillary side, although alveolar gas and blood are separated by an extremely thin membrane, and both alveolar epithelium and microcapillary endothelium are equally important compositions of the blood-gas interface (5). Indeed, histologic examination of emphysema lungs have shown that the alveolar septa in centrilobular emphysema appear to be remarkably thin and almost avas-

---

Received Jan. 10, 2003; revision accepted Jun. 10, 2003.

For correspondence or reprints contact: Noriaki Takabatake, MD, First Department of Internal Medicine, Yamagata University School of Medicine, 2-2-2, Iida-Nishi, Yamagata 990-9585, Japan.

E-mail: takabata@med.id.yamagata-u.ac.jp

cular, implying that vascular factors, such as a reduction of blood supply or functional defects of the pulmonary microcapillary vessels, might contribute to the progressive disappearance of lung tissue in patients with COPD (6).

Radioiodinated metaiodobenzylguanidine ( $^{123}\text{I}$ -metaiodobenzylguanidine [ $^{123}\text{I}$ -MIBG]), an analog of adrenergic neuron-blocking agent guanethidine, shares the same uptake, storage, and release mechanisms as norepinephrine in sympathetic nerve endings (7–11). Circulating biogenic amines, such as serotonin and norepinephrine, are actively taken up and metabolized by the lungs and have been used to evaluate the functional state of pulmonary endothelium in experimental models and in clinical conditions (12,13). The uptake mechanism of these amines includes a saturable, energy-requiring, sodium-dependent transport through pulmonary endothelial membrane. Because it has been demonstrated that  $^{123}\text{I}$ -MIBG is extracted by pulmonary endothelium with this transport system in the same manner as norepinephrine, noninvasive scintigraphic evaluation of  $^{123}\text{I}$ -MIBG kinetics in the lungs is considered to provide direct in vivo information of the functional state of pulmonary endothelium (14–18). Abnormal lung  $^{123}\text{I}$ -MIBG kinetics have been reported in the pathologic models of bleomycin-induced and endotoxin-induced lung injury, in which the presence of pulmonary microvascular injury plays a pivotal role in each condition (14,18). These findings further suggest that lung  $^{123}\text{I}$ -MIBG kinetics serve as a sensitive biochemical indicator of minimal endothelial cell lesions (14–18).

Against these backgrounds, we investigated the following: (a) whether lung  $^{123}\text{I}$ -MIBG kinetics in patients with COPD are significantly altered compared with those of healthy control subjects and (b) whether lung  $^{123}\text{I}$ -MIBG kinetics are significantly related to the clinical indices in patients with COPD. Elucidating these questions may provide novel insights into the involvement of the pulmonary microvascular injury in the pathogenesis of COPD, through the potential usefulness of lung  $^{123}\text{I}$ -MIBG kinetics in the in vivo evaluation of pulmonary endothelial cell dysfunction.

## MATERIALS AND METHODS

### Study Population

Twenty-five male patients with COPD were diagnosed according to the criteria established by the American Thoracic Society (19). Their irreversible chronic air-flow obstruction was confirmed by spiograms. The patients had been clinically stable for at least 3 mo and lacked clinical signs of exacerbation, such as acute respiratory infection. Patients with concomitant disease known to affect lung  $^{123}\text{I}$ -MIBG kinetics, such as diabetes mellitus or congestive heart failure, were excluded (20–22). All patients were former smokers.

Twelve age-matched healthy male volunteers were studied as control subjects. These control subjects had no medical illnesses and had normal physical examinations, laboratory data, and no history of cardiac disease. All were nonsmokers. None of the control subjects was taking any medications.

All subjects in this study had no record of hypertension, thyroid disease, or any drug therapy that could interfere with  $^{123}\text{I}$ -MIBG uptake (23). The clinical and lung  $^{123}\text{I}$ -MIBG scan data of the subjects, as well as information about the medical therapy the patients received, are shown in Table 1. The mean duration of the disease was  $9.9 \pm 7.7$  y (range, 1–27 y). The study protocol was approved by the local ethical committee of Yamagata University School of Medicine, and written informed consent was obtained from all subjects before participating in this study.

### Pulmonary Function Tests

Pulmonary function tests were performed with a CHESTAC-55V (Chest Corp.). Forced vital capacity (FVC), forced expiratory volume in 1 s ( $\text{FEV}_{1.0}$ ), residual volume (RV) using the helium dilution method, carbon monoxide diffusing capacity ( $\text{DL}_{\text{CO}}$ ), and alveolar volume ( $V_A$ ) using the single-breath method were measured. The ratio of  $\text{DL}_{\text{CO}}$  to  $V_A$  ( $\text{DL}_{\text{CO}}/V_A$ ) was expressed as the actual measurement values. FVC,  $\text{FEV}_{1.0}$ , and  $\text{DL}_{\text{CO}}/V_A$  were expressed as percentage of predicted values (% FVC, %  $\text{FEV}_{1.0}$ , and %  $\text{DL}_{\text{CO}}/V_A$ , respectively) according to the prediction equations of the Japanese Society of Chest Disease (24). Arterial blood gas was analyzed with the subject breathing room air in the supine position (pH, blood gas, electrolyte, glucose, and lactate analysis system 860COT; Bayer Medical Corp.).

### Imaging with $^{123}\text{I}$ -MIBG

$^{123}\text{I}$ -MIBG imaging was performed as reported previously with minor modifications (25,26). Briefly, 111 MBq  $^{123}\text{I}$ -MIBG (Daiichi Radioisotope Laboratories) were injected intravenously at resting supine position after overnight fasting. The radiochemical purity of  $^{123}\text{I}$ -MIBG was >96%. Anterior planar images were obtained over 10 min at 30 min (early image) and 270 min (delayed image) after the tracer injection. Imaging was performed with a  $\gamma$ -camera equipped with a low-energy, general-purpose collimator (ECAM; Siemens-Asahi Medical Technologies Ltd.), and the data were processed with an imaging processing system (ICON system; Siemens-Asahi Medical Technologies Ltd.). As shown in Figure 1, regions of interest (ROIs) were placed over superior mediastinum, upper right lung, and upper left lung to prevent scatter from liver and cardiac activity. Based on the average counts per pixel in each ROI, the uptake ratios of right lung to mediastinum (early image:  $\text{rt } L_E/M_E$ ; delayed image:  $\text{rt } L_D/M_D$ ) and left lung to mediastinum (early image:  $\text{lt } L_E/M_E$ ; delayed image:  $\text{lt } L_D/M_D$ ) were calculated. The mean uptake ratios of bilateral lungs to mediastinum of early image ( $(L/M)_E$ ) and delayed image ( $(L/M)_D$ ) were calculated as follows:

$$(L/M)_E = (\text{rt } L_E/M_E + \text{lt } L_E/M_E)/2,$$

$$(L/M)_D = (\text{rt } L_D/M_D + \text{lt } L_D/M_D)/2.$$

After correction for the acquisition time and decay of  $^{123}\text{I}$ ,  $^{123}\text{I}$ -MIBG washout rates between early image and delayed image of the right lung (rt WR) and the left lung (lt WR) were also calculated as follows:

$$\text{rt WR (\%)} = (\text{rt } L_E - \text{rt } L_D) \times 100/\text{rt } L_E,$$

$$\text{lt WR (\%)} = (\text{lt } L_E - \text{lt } L_D) \times 100/\text{lt } L_E.$$

The mean pulmonary washout rate (WR) of the  $^{123}\text{I}$ -MIBG of bilateral lungs was calculated as follows:

$$\text{WR (\%)} = (\text{rt WR (\%)} + \text{lt WR (\%)})/2,$$

**TABLE 1**  
Clinical and Scintigraphic Data of Patients with COPD and Control Subjects

Subject no.	Age (y)	Duration (y)	FEV <sub>1.0</sub> (L) (% predicted)	<sup>123</sup> I-MIBG scintigraphic data			Medical therapy		
				(L/M) <sub>E</sub>	(L/M) <sub>D</sub>	WR (%)	TP (mg)	OB (mg)	Steroid
COPD patients									
1	77	6	0.76 (34.7)	1.17	1.15	21.8	200	0.6	—
2	60	2	1.24 (43.4)	1.28	1.20	34.7	400	—	—
3	73	22	0.92 (43.8)	1.28	1.22	29.5	400	—	—
4	83	15	0.64 (40.5)	1.22	1.16	24.9	—	0.6	—
5	83	14	0.50 (36.5)	1.33	1.29	22.8	200	0.6	FP 800 μg
6	77	12	0.87 (40.7)	1.39	1.28	28.7	—	—	—
7	63	8	0.99 (36.7)	1.39	1.24	25.3	400	0.6	—
8	81	7	0.80 (48.2)	1.42	1.27	28.4	200	0.6	FP 800 μg
9	67	1	1.03 (49.3)	1.07	1.03	27.1	—	—	—
10	70	7	1.53 (64.6)	1.34	1.25	26.3	400	0.4	—
11	70	25	0.41 (17.8)	0.97	0.99	25.2	400	0.6	—
12	75	9	1.04 (52.8)	1.07	1.10	21.6	400	0.6	—
13	66	14	0.61 (30.8)	1.29	1.20	32.8	200	0.6	—
14	74	18	0.37 (16.6)	0.90	0.96	19.1	300	0.8	—
15	69	6	0.93 (40.3)	1.16	1.21	22.3	400	—	MP 4 mg
16	44	5	0.88 (24.8)	1.35	1.21	38.1	—	0.4	FP 400 μg
17	79	5	0.74 (42.0)	1.22	1.14	29.5	400	0.8	—
18	74	27	0.51 (24.4)	1.46	1.32	34.9	200	0.6	MP 4 mg
19	77	3	1.19 (54.6)	1.10	1.09	24.0	200	0.6	—
20	73	12	0.57 (32.4)	1.12	1.08	30.9	400	—	FP 400 μg
21	75	2	2.19 (104.3)	1.69	1.50	32.8	200	0.6	—
22	74	5	1.08 (51.9)	1.53	1.37	36.5	400	0.8	—
23	79	20	0.73 (36.5)	1.35	1.28	20.4	400	—	PSL 7.5 mg
24	74	1	2.63 (122.3)	1.22	1.21	21.9	—	—	—
25	77	1	0.74 (37.6)	1.28	1.25	25.6	—	—	—
Control subjects									
1	52	—	3.67 (115.8)	1.71	1.43	39.1	—	—	—
2	75	—	1.61 (95.3)	1.51	1.28	24.6	—	—	—
3	73	—	2.23 (119.3)	1.54	1.30	43.9	—	—	—
4	66	—	3.1 (127.0)	1.65	1.34	40.0	—	—	—
5	87	—	2.78 (178.2)	1.52	1.41	29.3	—	—	—
6	82	—	2.42 (114.7)	1.46	1.31	26.7	—	—	—
7	78	—	2.81 (126.6)	1.52	1.25	32.1	—	—	—
8	73	—	2.44 (117.3)	1.60	1.32	36.8	—	—	—
9	73	—	3.42 (155.5)	1.37	1.21	32.7	—	—	—
10	64	—	3.34 (126.5)	1.65	1.51	31.1	—	—	—
11	50	—	3.90 (127.5)	1.66	1.38	38.0	—	—	—
12	67	—	2.81 (121.1)	1.36	1.25	35.9	—	—	—

(L/M)<sub>E</sub> = mean uptake ratio of <sup>123</sup>I-MIBG of bilateral lungs to mediastinum in early image; (L/M)<sub>D</sub> = mean uptake ratio of <sup>123</sup>I-MIBG of bilateral lungs to mediastinum in delayed image; WR = mean washout rate of <sup>123</sup>I-MIBG of bilateral lungs between early and delayed image; TP = oral administration of theophylline per day; OB = inhaled administration of oxitropium bromide per day; FP = inhaled administration of fluticasone propionate per day; MP = oral administration of methylprednisolone per day; PSL = oral administration of prednisolone per day.

where M, rt L, lt L, and L represent the counts at the mediastinum, right lung, left lung, and whole lung; E and D indicate early image and delayed image, respectively.

### CT Scans

The CT scans were performed in the supine position using a high-resolution CT scanner (HiSpeed Advantage; GE Yokogawa Medical System) with 1-mm collimation, scanning time of 1.0 s, 120-kV electrical voltage, 200-mA electrical current, and 34.5-cm field of view. A high-resolution reconstruction algorithm for the

lung was used (Bone; GE Yokogawa Medical System). High-resolution CT images were taken at deep inspiration. No contrast medium was injected. A section of the superior margin of the aortic arch was used for the analysis, because this section was coincident with the <sup>123</sup>I-MIBG scanning area. The CT image was composed of a 512 × 512 matrix of numeric data (CT numbers) in Hounsfield units (HU). The percentage ratio of low-attenuation area (LAA) to the corresponding lung area (% LAA) was calculated automatically as reported previously with minor modifications (27–29). The cutoff level between the

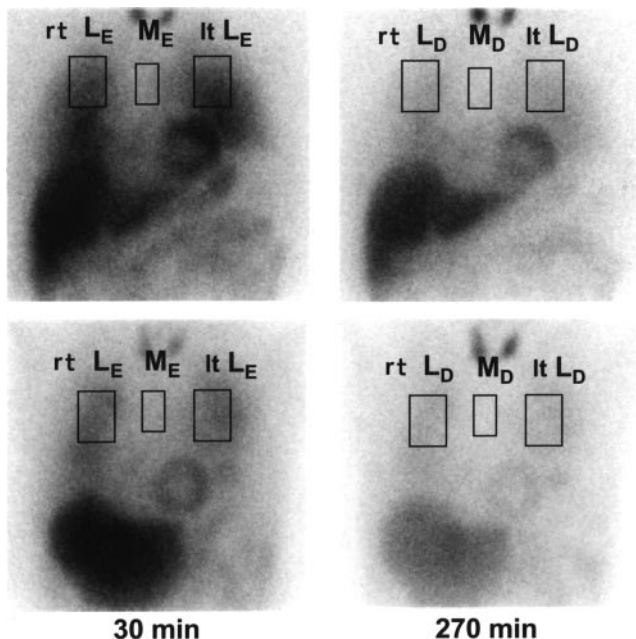


**FIGURE 1.** Anterior planar images of lung  $^{123}\text{I}$ -MIBG scintigraphy (left, early images; right, delayed images) in representative control subject (Top) and COPD patient (Bottom). M, rt L, and lt L represent counts in ROIs at mediastinum, right lung, and left lung; E and D indicate early images (at 30 min after intravenous injection of  $^{123}\text{I}$ -MIBG) and delayed images (at 270 min after intravenous injection of  $^{123}\text{I}$ -MIBG), respectively. Note that rt L<sub>E</sub>, rt L<sub>D</sub>, lt L<sub>E</sub>, and lt L<sub>D</sub>, as well as washout rate (WR) between early and delayed images, are lower in COPD patient than in control subject.

normal lung density area and the LAA was defined as  $-960$  HU (27–29).

### Statistical Analysis

A Mann–Whitney *U* test for nonparametric data was used to analyze the difference between the 2 groups. The relations between continuous variables were evaluated by Spearman rank correlations. Results are expressed as mean  $\pm$  SD. Significance was determined at the 5% level. Statistical analysis was done using the Statview Statistical Package (Statview, Inc.) (30).

## RESULTS

### Characteristics of Study Population

Clinical characteristics of both the COPD patients and the healthy control subjects are summarized in Table 2. The COPD patients showed fixed air-flow obstruction defined as an FEV<sub>1.0</sub>/FVC ratio of  $<70\%$  without response to bronchodilators. None of the patients had large bullae or other lung disease. The % FVC, % FEV<sub>1.0</sub>, and % DL<sub>CO</sub>/V<sub>A</sub> values of the COPD patients were significantly lower than those of the healthy control subjects. The COPD patients were associated with decreased arterial blood oxygen pressure (PaO<sub>2</sub>) and increased arterial blood carbon dioxide pressure (Paco<sub>2</sub>). Alveolar–arterial oxygen tension gradient ([A–a]DO<sub>2</sub>) levels of the COPD patients were significantly higher than those of the healthy control subjects. The %

**TABLE 2**  
Characteristics of Study Population

Characteristic	COPD patients (n = 25)	Control subjects (n = 12)	P value*
Age (y)	72.6 $\pm$ 8.3	70.0 $\pm$ 11.0	NS
FVC (L)	2.25 $\pm$ 0.77	3.63 $\pm$ 0.72	$<0.0001$
% FVC	71.1 $\pm$ 22.3	112.0 $\pm$ 15.9	$<0.0001$
FEV <sub>1.0</sub> (L)	0.96 $\pm$ 0.52	2.88 $\pm$ 0.65	$<0.0001$
% FEV <sub>1.0</sub>	45.1 $\pm$ 23.5	127.1 $\pm$ 21.1	$<0.0001$
FEV <sub>1.0</sub> /FVC (%)	41.6 $\pm$ 10.9	79.0 $\pm$ 4.4	$<0.0001$
DL <sub>CO</sub> /V <sub>A</sub> (mL/min/mm Hg/L)	2.43 $\pm$ 1.07	3.67 $\pm$ 1.07	$<0.01$
% DL <sub>CO</sub> /V <sub>A</sub>	56.2 $\pm$ 24.6	82.3 $\pm$ 19.2	$<0.01$
Arterial PO <sub>2</sub> (mm Hg)	67.4 $\pm$ 12.3	83.4 $\pm$ 9.8	$<0.01$
Arterial PCO <sub>2</sub> (mm Hg)	47.7 $\pm$ 7.4	41.9 $\pm$ 2.1	$<0.01$
[A–a]DO <sub>2</sub> (mm Hg)	25.2 $\pm$ 11.2	16.1 $\pm$ 10.1	$<0.05$
% LAA	15.5 $\pm$ 12.0	2.7 $\pm$ 4.3	$<0.0001$

\*Mann–Whitney *U* test.

NS = not significant; % FVC = percentage of predicted values of FVC; % FEV<sub>1.0</sub> = percentage of predicted values of FEV<sub>1.0</sub>; % DL<sub>CO</sub>/V<sub>A</sub> = percentage of predicted values of DL<sub>CO</sub>/V<sub>A</sub>; [A–a]DO<sub>2</sub> = alveolar–arterial oxygen tension gradient; % LAA = percentage ratio of low-attenuation area to corresponding lung area.

Values are presented as mean  $\pm$  SD.

LAA values of the COPD patients were significantly higher than those of the healthy control subjects.

### Pulmonary $^{123}\text{I}$ -MIBG Kinetics of Study Population

(L/M)<sub>E</sub>, (L/M)<sub>D</sub>, and lung WR of the  $^{123}\text{I}$ -MIBG of the study population are shown in Table 3. (L/M)<sub>E</sub> and (L/M)<sub>D</sub> were significantly lower in the COPD patients than in the control subjects. In addition, WR was significantly reduced in the COPD patients compared with the control subjects. The less profound decrease of (L/M)<sub>D</sub> ( $-9.8\%$ ) versus (L/M)<sub>E</sub> ( $-18.2\%$ ) in COPD patients, compared with control subjects, is due to the relative reduction of WR of the tracer in COPD patients.

In light of the ability of lung WR of the  $^{123}\text{I}$ -MIBG—which is independent of an alteration of the pulmonary vascular surface area—to indicate the ongoing pulmonary endothelial dysfunction (20–22,31), we next evaluated the relationships between lung WR of the  $^{123}\text{I}$ -MIBG and other

**TABLE 3**  
Scintigraphic Study Results

Parameter	COPD patients (n = 25)	Control subjects (n = 12)	P value*
(L/M) <sub>E</sub>	1.26 $\pm$ 0.18	1.54 $\pm$ 0.11	$<0.0001$
(L/M) <sub>D</sub>	1.20 $\pm$ 0.12	1.33 $\pm$ 0.09	$<0.001$
WR (%)	27.4 $\pm$ 5.3	34.2 $\pm$ 5.7	$<0.01$

\*Mann–Whitney *U* test.

Values are presented as mean  $\pm$  SD.

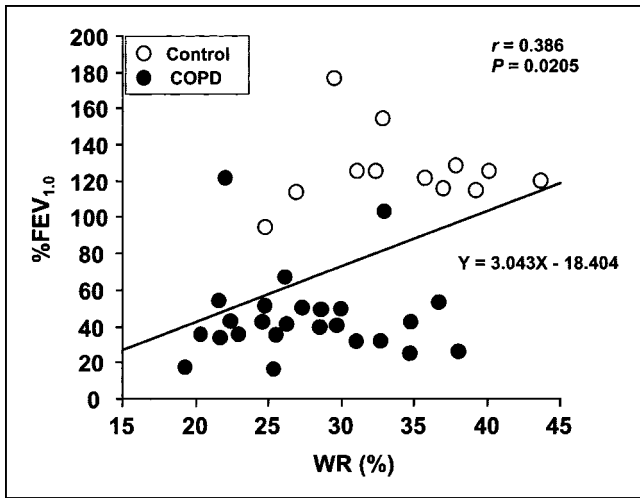


**FIGURE 2.** Relationship between % FEV<sub>1.0</sub> and lung WR of <sup>123</sup>I-MIBG (%) in study population. There is significant positive correlation between them ( $r = 0.386$ ,  $P < 0.05$ ). ●, COPD patients; ○, control subjects.

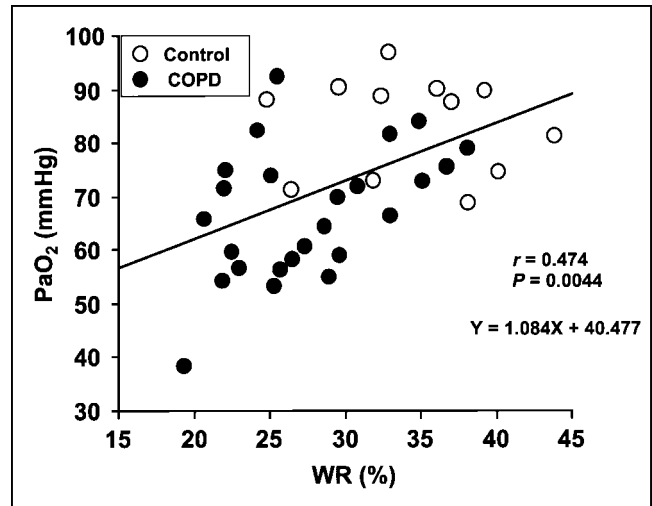


**FIGURE 4.** Relationship between PaO<sub>2</sub> (mm Hg) and lung WR of <sup>123</sup>I-MIBG (%) in study population. There is significant positive correlation between them ( $r = 0.474$ ,  $P < 0.01$ ). ●, COPD patients; ○, control subjects.

diagnostic tests for the severity of COPD. There were significant positive correlations between WR and % FEV<sub>1.0</sub> ( $r = 0.386$ ,  $P < 0.05$ ; Fig. 2), DL<sub>CO</sub>/V<sub>A</sub> ( $r = 0.449$ ,  $P < 0.01$ ; Fig. 3), and PaO<sub>2</sub> ( $r = 0.474$ ,  $P < 0.01$ ; Fig. 4). In contrast, there were significant inverse correlations between WR and [A-a]DO<sub>2</sub> ( $r = -0.446$ ,  $P < 0.01$ ; Fig. 5) and % LAA ( $r = -0.458$ ,  $P < 0.01$ ; Fig. 6).

In addition, when only COPD patients were compared, similar significant correlations were observed between WR and DL<sub>CO</sub>/V<sub>A</sub> ( $r = 0.401$ ,  $P < 0.05$ ; Fig. 3), PaO<sub>2</sub> ( $r = 0.430$ ,  $P < 0.05$ ; Fig. 4), [A-a]DO<sub>2</sub> ( $r = -0.483$ ,  $P < 0.05$ ; Fig. 5), and % LAA ( $r = -0.439$ ,  $P < 0.05$ ; Fig. 6). These correlations were not observed in the control subjects.

## DISCUSSION

The lung actively takes up <sup>123</sup>I-MIBG through a saturable, energy-requiring, sodium-dependent transport mechanism similar to biogenic amines (14–18). Previous studies confirmed the diagnostic value of <sup>123</sup>I-MIBG as an excellent marker in recognizing minimal endothelial cell lesions (14–18,20–22,31–33). Since transport of biogenic amines by pulmonary endothelium requires normal endothelial cell integrity, reports have shown that pulmonary uptake of <sup>123</sup>I-MIBG, as well as its washout, is a suitable indicator of endothelial function, and decreases in these values reflect endothelial cell injury (14–18,20–22,31–33). In this study, we demonstrated that both the lung uptake of <sup>123</sup>I-MIBG

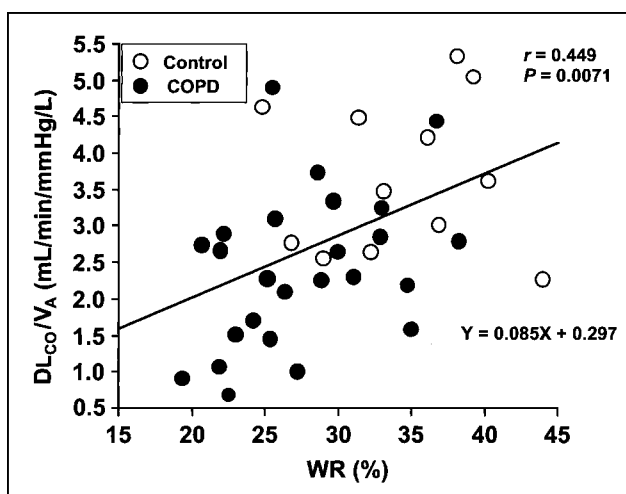


**FIGURE 3.** Relationship between DL<sub>CO</sub>/V<sub>A</sub> (mL/min/mm Hg/L) and lung WR of <sup>123</sup>I-MIBG (%) in study population. There is significant positive correlation between them ( $r = 0.449$ ,  $P < 0.01$ ). ●, COPD patients; ○, control subjects.

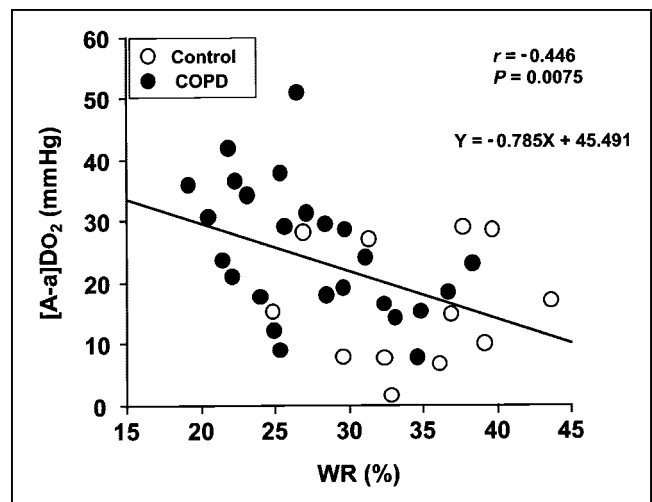


**FIGURE 5.** Relationship between [A-a]DO<sub>2</sub> (mm Hg) and lung WR of <sup>123</sup>I-MIBG (%) in study population. There is significant inverse correlation between them ( $r = -0.446$ ,  $P < 0.01$ ). ●, COPD patients; ○, control subjects.

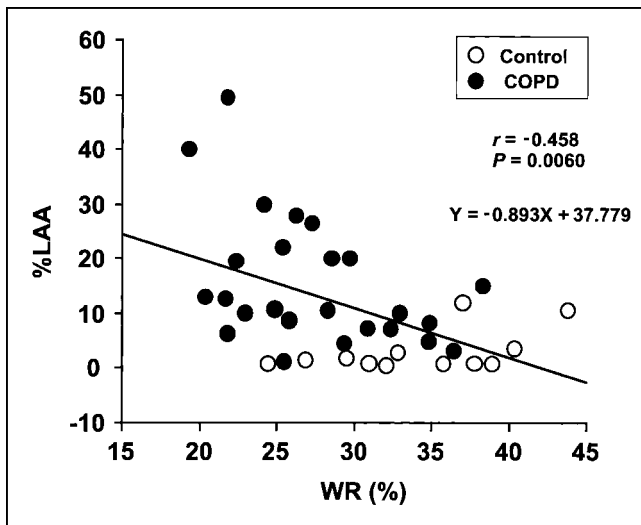


**FIGURE 6.** Relationship between % LAA and lung WR of  $^{123}\text{I}$ -MIBG (%) in study population. There is significant inverse correlation between them ( $r = -0.458$ ,  $P < 0.01$ ). ●, COPD patients; ○, control subjects.

and its WR in patients with COPD were significantly reduced compared with those of the control subjects and that there were significant correlations between lung WR of  $^{123}\text{I}$ -MIBG and other diagnostic tests for the severity of COPD, such as % FEV<sub>1.0</sub>, DL<sub>CO</sub>/V<sub>A</sub>, PaO<sub>2</sub>, [A-a]DO<sub>2</sub>, and % LAA. These results may suggest that endothelial cell injury in the pulmonary capillaries and small venules are involved in the pathogenesis of COPD and that these microvascular endothelial lesions, at least in part, play a significant role in the progression of COPD.

It is known that lung  $^{123}\text{I}$ -MIBG kinetics differ according to the nature of the disease. In the lung toxicity of bleomycin and endotoxemia, decreased lung uptake of  $^{123}\text{I}$ -MIBG has been noted and attributed to intracytoplasmic edema and blebbing of the endothelial cells, both detected by electron microscopy (14,18). However, it has been reported that lung uptake of  $^{123}\text{I}$ -MIBG is also dependent on the pulmonary vascular surface area, which is accessible to the blood pool (17). Therefore, it can be speculated that changes in pulmonary circulation involving the alterations of both the vascular surface area (loss of the pulmonary vascular bed due to emphysematous change) and the endothelial cell function are responsible for the decreased lung uptake of  $^{123}\text{I}$ -MIBG in COPD patients. In contrast, lung WR of  $^{123}\text{I}$ -MIBG is considered to be independent of an alteration of the pulmonary vascular surface area, because it indicates the absolute decline in counts between early and delayed image. Reduced lung WR of  $^{123}\text{I}$ -MIBG and its relation to the severity of the disease have been reported in patients with diabetes mellitus and with Bechet's disease, in which the presence of pulmonary microangiopathy and pulmonary microvascular injury, respectively, play an important role in the pulmonary complication in each disease (20,21,31). In this study, we demonstrated that there were significant correlations be-

tween lung WR of  $^{123}\text{I}$ -MIBG and other diagnostic tests for the severity of COPD. Taken together, lung WR of  $^{123}\text{I}$ -MIBG, but not its uptake, is considered a true indicator of the functional status of the pulmonary endothelial cells in patients with COPD.

Smooth muscles, mucous glands, and blood vessels of the respiratory tract in the lungs are dominated by autonomic nerves.  $^{123}\text{I}$ -MIBG shares the same uptake, storage, and release mechanisms as norepinephrine in sympathetic nerve endings (7-11). Therefore, lung  $^{123}\text{I}$ -MIBG kinetics may be related not only to the number of pulmonary endothelial cells and the degree of their injury but also to many other factors, such as distribution of sympathetic nerves and its functional status in the pulmonary blood vessels and bronchus. Sympathovagal imbalance of the autonomic nerves in the pulmonary microvascular walls may produce an additional interference leading to changes in lung  $^{123}\text{I}$ -MIBG kinetics observed in COPD patients, because we previously observed systemic abnormalities of the autonomic nervous system in patients with COPD (34,35). Furthermore, WR tends to decrease when the flow rate of the blood becomes small. The decline of lung WR of  $^{123}\text{I}$ -MIBG in patients with COPD can be attributed to the endothelial damages, but their contribution to the decrease in WR might be limited, and the reduced pulmonary perfusion due to an inhomogeneous loss of lung parenchyma (emphysematous change) might play a role in the WR decrease in patients with COPD.

In this study, we demonstrated that there were significant correlations between lung WR of  $^{123}\text{I}$ -MIBG and other diagnostic tests for the severity of COPD. However, % FEV<sub>1.0</sub> and % LAA are thought to be closely related to the microscopic architecture of the lung and, thus, may not be related to the microvascular endothelial cell damage. In contrast, DL<sub>CO</sub>/V<sub>A</sub>, PaO<sub>2</sub>, and [A-a]DO<sub>2</sub> are all related to the permeability of alveolar surface to CO and O<sub>2</sub>—namely, to diffusion capacity. In addition, there were similar significant relationships between WR and these diffusion capacity-related parameters when only COPD patients were compared. Although there are many reasons for the decrease in diffusion capacity (i.e., loss of pulmonary vascular bed or thickening of the alveolar wall) and, therefore, the microvascular endothelial damage could not be the only reason for the decrease of diffusion capacity, lung WR of  $^{123}\text{I}$ -MIBG could also be used as an indicator for the impairment of diffusion capacity commonly observed in patients with COPD.

Scintigraphic results of this study showed wide spreading of the data in different patients (i.e., the SD for lung WR of  $^{123}\text{I}$ -MIBG in COPD patients is approximately 19% of the mean [Table 3]). Moreover, the comparison between lung WR of  $^{123}\text{I}$ -MIBG and other diagnostic tests for the severity of COPD showed the presence of high overlapping of the value between COPD patients and control subjects (Figs. 2-6). These results are not inexplicable, because the COPD patients recruited in this study have a wide variety of

disease status and backgrounds, such as the severity of the disease (as expressed by the % FEV<sub>1.0</sub> values) and the history of the disease, both of which are shown in Table 1.

Patients with COPD exhibit heterogeneous pulmonary perfusion due to an inhomogeneous loss of lung parenchyma. This inhomogeneous pulmonary perfusion causes the decrease in PaO<sub>2</sub> and the increase in [A-a]Do<sub>2</sub> mainly by ventilation-perfusion inequality (mismatching of ventilation and blood flow) in the small alveolar-capillary units. However, this heterogeneous pulmonary perfusion does not have an influence on the WR calculation, as long as <sup>123</sup>I-MIBG scanning is performed over the same ROI in the same patient between early and delayed image. In addition, WR is calculated as follows:  $WR (\%) = (L_E - L_D) \times 100/L_E$ , where L indicates mean counts per pixel in each ROI. Because we draw a substantially large scanning field as each ROI, the effect of regionally inhomogeneous pulmonary perfusion in the small alveolar-capillary units on the WR can be ignored.

Although the underlying mechanisms of the pulmonary endothelial cell dysfunction demonstrated in our COPD patients are difficult to explain, several speculations warrant further discussion. First, hypoxemia observed in COPD patients is known to cause spasms of the fine arterioles, leading to the higher pulmonary artery pressure (36). Stress studies have demonstrated that pulmonary endothelium exposed to high transmural pressure undergoes ultrastructural changes followed by the disruption of the capillary endothelium (37,38). Although we did not measure the pulmonary artery pressure in this study, this possibility seems to be likely, because we found a significant positive correlation between lung WR of <sup>123</sup>I-MIBG and PaO<sub>2</sub> levels in the study population (Fig. 4). Second, a chronic inflammatory process, including cytokine activation, occurring in alveolar air spaces, may have influence on the functional defects or injuries of the pulmonary microcapillary endothelium because of the particularly intimate contact of the delicate alveolar-capillary unit and the predominance of the composition of pulmonary capillaries in the alveolar walls (i.e., >75% of the total alveolar wall in volume) (5). Third, Kasahara et al. recently reported the finding of enhanced endothelial cell apoptosis due to decreased expression of vascular endothelial growth factor and its receptor 2 in emphysema lung and pointed out that vascular factors might have a role in the pathogenesis of COPD (39,40). Their finding further supports our results of the direct in vivo evidence of the pulmonary endothelial cell lesions demonstrated by the abnormal lung <sup>123</sup>I-MIBG kinetics in patients with COPD.

In summary, we evaluated pulmonary <sup>123</sup>I-MIBG kinetics and other clinical indices in clinically stable patients with COPD and age-matched healthy control subjects. We demonstrated that both the lung uptake of <sup>123</sup>I-MIBG and its WR in patients with COPD were significantly reduced compared with those of the control subjects. We also showed that there were significant correlations between lung WR of <sup>123</sup>I-

MIBG and other diagnostic tests for the severity of COPD, such as % FEV<sub>1.0</sub>, DL<sub>CO</sub>/V<sub>A</sub>, PaO<sub>2</sub>, [A-a]Do<sub>2</sub>, and % LAA. Although there is a limitation due to the high cost of this tracer, the results of this study may suggest that lung WR of <sup>123</sup>I-MIBG, unlike any other pulmonary function tests analyzed in this study, is a reliable and specific biochemical marker of endothelial cell dysfunction in patients with COPD and that this valuable tool provides direct in vivo evidence of the involvement of the pulmonary microvascular injury in the pathogenesis of COPD.

## CONCLUSION

Pulmonary microvascular endothelial cell injury is involved in the pathogenesis of COPD, and lung scintigraphic assessment of <sup>123</sup>I-MIBG, which reflects latent microvascular endothelial damage, can be a new diagnostic tool to evaluate the functional severity of COPD.

## ACKNOWLEDGMENT

This study was supported in part by grants-in-aid for Scientific Research (11557044 and 13770295) from the Ministry of Education, Culture, Sports, Science and Technology, Japan.

## REFERENCES

1. Murray CJL, Lopez AD. Evidence-based health policy: lessons from the global burden of disease study. *Science*. 1996;274:740-743.
2. Pauwels RA, Buist AS, Calverley PMA, Jenkins CR, Hurd SS, on behalf of the GOLD Scientific Committee. Global strategy for the diagnosis, management, and prevention of chronic obstructive pulmonary disease: National Heart, Lung, and Blood Institute and World Health Organization global initiative for chronic obstructive lung disease (GOLD)—workshop summary. *Am J Respir Crit Care Med*. 2001;163:1256-1276.
3. Barnes PJ. Chronic obstructive pulmonary disease. *N Engl J Med*. 2000;343:269-280.
4. Piquette CA, Rennard SI, Snider GL. Chronic bronchitis and emphysema. In: Murray JF, Nadel JA, eds. *Textbook of Respiratory Medicine*. 3rd ed. Philadelphia, PA: WB Saunders; 2000:1187-1245.
5. Albertine KH, Williams MC, Hyde DM. Anatomy of the lungs. In: Murray JF, Nadel JA, eds. *Textbook of Respiratory Medicine*. 3rd ed. Philadelphia, PA: WB Saunders; 2000:3-33.
6. Liebow AA. Pulmonary emphysema with special reference to vascular changes. *Am Rev Respir Dis*. 1959;80:67-93.
7. Wieland DM, Wu J, Brown LE, Mangner TJ, Swanson DP, Beierwaltes WH. Radiolabeled adrenergic neuron-blocking agents: adrenomedullary imaging with [<sup>131</sup>I]iodobenzylguanidine. *J Nucl Med*. 1980;21:349-353.
8. Wieland DM, Brown LE, Rogers WL, et al. Myocardial imaging with a radioiodinated norepinephrine storage analog. *J Nucl Med*. 1981;22:22-31.
9. Wieland DM, Brown LE, Tobes MC, et al. Imaging the primate adrenal medulla with [<sup>123</sup>I] and [<sup>131</sup>I] meta-iodobenzylguanidine: concise communication. *J Nucl Med*. 1981;22:358-364.
10. Tobes MC, Jaques S Jr, Wieland DM, Sisson JC. Effect of uptake-one inhibitors on the uptake of norepinephrine and metaiodobenzylguanidine. *J Nucl Med*. 1985;26:897-907.
11. Sisson JC, Wieland DM, Sherman P, Mangner TJ, Tobes MC, Jacques S Jr. Metaiodobenzylguanidine as an index of the adrenergic nervous system integrity and function. *J Nucl Med*. 1987;28:1620-1624.
12. Gillis CN, Pitt BR. The fate of circulating amines within the pulmonary circulation. *Ann Rev Physiol*. 1982;44:269-281.
13. Gillis CN. Pharmacological aspects of metabolic processes in the pulmonary microcirculation. *Ann Rev Pharmacol Toxicol*. 1986;26:183-200.
14. Slosman DO, Davidson D, Brill AB, Alderson PO. <sup>131</sup>I-Metaiodobenzylguanidine uptake in the isolated rat lung: a potential marker of endothelial cell function. *Eur J Nucl Med*. 1988;13:543-547.
15. Slosman DO, Morel DR, Mo Costabella PM, Donath A. Lung uptake of <sup>131</sup>I-

- metaiodobenzylguanidine in sheep: an in vivo measurement of pulmonary metabolic function. *Eur J Nucl Med*. 1988;14:65–70.
16. Slosman DO, Morel DR, Alderson PO. A new imaging approach to quantitative evaluation of pulmonary vascular endothelial metabolism. *J Thorac Imaging*. 1988;3:49–52.
  17. Slosman DO, Donath A, Alderson PO. <sup>131</sup>I-Metaiodobenzylguanidine and <sup>125</sup>I-iodoamphetamine: parameters of lung endothelial cell function and pulmonary vascular area. *Eur J Nucl Med*. 1989;15:207–210.
  18. Slosman DO, Polla BS, Donath A. <sup>123</sup>I-MIBG pulmonary removal: a biochemical marker of minimal lung endothelial cell lesions. *Eur J Nucl Med*. 1990;16:633–637.
  19. American Thoracic Society. Standards for the diagnosis and care of patients with chronic obstructive pulmonary disease. *Am J Respir Crit Care Med*. 1995;152: S77–S120.
  20. Murashima S, Takeda K, Matsumura K, et al. Increased lung uptake of iodine-123-MIBG in diabetics with sympathetic nervous dysfunction. *J Nucl Med*. 1998;39:334–338.
  21. Unlu M, Inanir S. Prolonged lung retention of iodine-123-MIBG in diabetic patients. *J Nucl Med*. 1998;39:116–118.
  22. Mu X, Hasegawa S, Yoshioka J, et al. Clinical value of lung uptake of iodine-123 metaiodobenzylguanidine (MIBG), a myocardial sympathetic nerve imaging agent, in patients with chronic heart failure. *Ann Nucl Med*. 2001;15:411–416.
  23. Solanki KK, Bomanji J, Moyes J, Mather SJ, Trainer PJ, Britton KE. A pharmacological guide to medicines which interfere with the biodistribution of radiolabelled metaiodobenzylguanidine (MIBG). *Nucl Med Commun*. 1992;13: 513–521.
  24. Japanese Society of Chest Disease. Standards of pulmonary function tests for Japanese. *Jpn J Thorac Dis*. 1993;31:appendix.
  25. Takeishi Y, Atsumi H, Fujiwara S, Takahashi K, Tomoike H. ACE inhibition reduces cardiac iodine-123-MIBG release in heart failure. *J Nucl Med*. 1997;38: 1085–1089.
  26. Atsumi H, Takeishi Y, Fujiwara S, Tomoike H. Cardiac sympathetic nervous disintegrity is related to exercise intolerance in patients with chronic heart failure. *Nucl Med Commun*. 1998;19:451–456.
  27. Sakai N, Mishima M, Nishimura K, Itoh H, Kuno K. An automated method to assess the distribution of low attenuation areas on chest CT scans in chronic pulmonary emphysema patients. *Chest*. 1994;106:1319–1325.
  28. Mishima M, Oku Y, Kawakami K, et al. Quantitative assessment of the spatial distribution of low attenuation areas on x-ray CT using texture analysis in patients with chronic pulmonary emphysema. *Front Med Biol Eng*. 1997;8:19–34.
  29. Mishima M, Hirai T, Jin Z, et al. Standardization of low attenuation area versus total lung area in chest x-ray CT as an indicator of chronic pulmonary emphysema. *Front Med Biol Eng*. 1997;8:79–86.
  30. Takabatake N, Nakamura H, Abe S, et al. The relationship between chronic hypoxemia and activation of the tumor necrosis factor- $\alpha$  system in patients with chronic obstructive pulmonary disease. *Am J Respir Crit Care Med*. 2000;161: 1179–1184.
  31. Unlu M, Akincioglu C, Yamac K, Onder M. Pulmonary involvement in Behcet's disease: evaluation of <sup>123</sup>I-MIBG retention. *Nucl Med Commun*. 2001;22:1083–1088.
  32. Richalet JP, Merlet P, Bourguignon M, et al. MIBG scintigraphic assessment of cardiac adrenergic activity in response to altitude hypoxia. *J Nucl Med*. 1990; 31:34–37.
  33. Koizumi T, Kubo K, Hanaoka M, et al. Serial scintigraphic assessment of iodine-123 metaiodobenzylguanidine lung uptake in a patient with high-altitude pulmonary edema. *Chest*. 1999;116:1129–1131.
  34. Takabatake N, Nakamura H, Abe S, et al. Circulating leptin in patients with chronic obstructive pulmonary disease. *Am J Respir Crit Care Med*. 1999;159: 1215–1219.
  35. Takabatake N, Nakamura H, Minamihaba O, et al. A novel pathophysiologic phenomenon in cachexic patients with chronic obstructive pulmonary disease: the relationship between the circadian rhythm of circulating leptin and the very low-frequency component of heart rate variability. *Am J Respir Crit Care Med*. 2001;163:1314–1319.
  36. Malik AB, Vogel SM, Minshall RD, Tirupathi C. Pulmonary circulation and regulation of fluid balance. In: Murray JF, Nadel JA, eds. *Textbook of Respiratory Medicine*. 3rd ed. Philadelphia, PA: WB Saunders; 2000:119–154.
  37. West JB, Tsukimoto K, Mathieu-Costello O, Prediletto R. Stress failure in pulmonary capillaries. *J Appl Physiol*. 1991;70:1731–1742.
  38. Tsukimoto K, Mathieu-Costello O, Prediletto R, Elliott AR, West JB. Ultrastructural appearances of pulmonary capillaries at high transmural pressures. *J Appl Physiol*. 1991;71:573–582.
  39. Kasahara Y, Tuder RM, Taraseviciene-Stewart L, et al. Inhibition of VEGF receptors causes lung cell apoptosis and emphysema. *J Clin Invest*. 2000;106: 1311–1319.
  40. Kasahara Y, Tuder RM, Cool CD, Lynch DA, Flores SC, Voelkel NF. Endothelial cell death and decreased expression of vascular endothelial growth factor and vascular endothelial growth factor receptor 2 in emphysema. *Am J Respir Crit Care Med*. 2001;163:737–744.